Validating Atmospheric Reanalysis Data Using Tropical Cyclones as Thermometers

James P. Kossin
NOAA National Climatic Data Center, Asheville, NC, USA

Mailing address:
NOAA Cooperative Institute for Meteorological Satellite Studies, 1225 West Dayton Street, Madison, WI 53706 USA (james.kossin@noaa.gov)

Preliminary Accepted Version in the Bulletin of the American Meteorological Association (Received 11 August 2014; accepted 15 October 2014)

If you would like to cite the Early Online Release in a separate work, please use the following full citation:

Kossin, J. P., 2014: Validating atmospheric reanalysis data using tropical cyclones as thermometers. *Bull. Amer. Meteor. Soc.* doi:10.1175/BAMS-D-14-00180, in press.

Capsule

Tropical cyclones are used as traveling thermometers to globally sample upper-tropospheric temperatures and help mitigate uncertainties due to discrepancies among different reanalysis data products.

Abstract

Temperatures in the upper-troposphere of the atmosphere, near the tropopause, play a key role in the evolution of tropical cyclones (TC) by controlling their potential intensity (PI), which describes the thermodynamically-based maximum TC intensity that the environment will support. Accurately identifying past trends in PI is critical for understanding the causes of observed changes in TC intensity, but calculations of PI trends using different atmospheric reanalysis products can give very different results, due largely to differences in their representation of upper-tropospheric temperatures. Without a means to verify the fidelity of the upper-tropospheric temperatures, PI trends calculated from these products are very uncertain.

Here, a method is introduced to validate the upper-tropospheric temperatures in the reanalysis products by using the TCs themselves as thermometers. Using a 30-year global dataset of TC cloud-top temperatures, and three widely-utilized atmospheric reanalysis products – MERRA, ERA-Interim, and NCEP/NCAR – it is shown that storm-local upper-level temperatures in the MERRA and ERA-Interim data vary similarly to the TC cloud-top temperatures on both interannual and decadal timescales, but the NCEP/NCAR data have substantial biases that introduce an increasing trend in storm-local PI not found in the other two products. The lack of global storm-local PI trends is due to a balance between temporal increases in the mean state and the poleward migration of TCs into lower climatological PI, and has significant implications for the detection and attribution of mean TC intensity trends.

Introduction

The question of how tropical climate variability and change has affected and will affect tropical cyclones has been the subject of intensive study (Knutson et al. 2010; Seneviratne et al. 2012; Christensen, et al. 2013). Theory and numerical modeling simulations suggest that increases in the mean potential intensity (Bister and Emanuel 1998; Emanuel 1999) of the environment through which tropical cyclones track will cause mean tropical cyclone intensity to increase (Emanuel 2000; Kossin et al. 2013). Potential intensity describes the thermodynamically-based maximum tropical cyclone intensity that the environment will support, all other factors being optimal, and is strongly correlated with temperatures near the tropopause (Emanuel et al. 2013; Vecchi et al. 2013) as well as sea surface temperature, which affects potential intensity directly and indirectly through the difference between sea surface temperature and the temperature of the free troposphere (Emanuel et al. 2013).

Past variability and trends in air temperature and potential intensity are typically explored with atmospheric reanalysis products, such as the Modern-Era Retrospective Analysis for Research and Applications (MERRA; Rienecker et al. 2011), the European Centre for Medium-Range Weather Forecasting Interim Re-Analysis (ERA-Interim; Dee et al. 2011), and the National Centers for Environmental Prediction / National Center for Atmospheric Research Global Reanalysis 1 (NCEP/NCAR; Kalnay et al. 1996). But potential intensity trends calculated from these products can differ substantially from each other (Fig. 1). For example, in the period 1980–2010, the NCEP/NCAR data in general exhibit much larger increases in potential intensity than the MERRA or ERA-Interim data, and in some regions there is even disagreement in the sign of the change. These differences have been shown to be largely due to differences in upper-tropospheric temperatures among the products (Emanuel et al. 2013; Vecchi et al. 2013), and they introduce substantial uncertainty into the changes in tropical cyclone intensity that would be theoretically expected over this period. For example, if tropical cyclones have not been experiencing long-term increases in their mean local potential intensity, then there is no obvious expectation for detecting increasing trends in their mean intensity, at least within the constructs of potential intensity theory.

Here, a method is introduced to help validate the upper-tropospheric temperatures in the reanalysis products by using the tropical cyclones themselves as thermometers. Because tropical cyclones maintain vigorous and persistent updrafts near their centers that reach the tropopause, the cloud-top temperatures of the resulting clouds, which can be measured directly with infrared sensors on satellites, serve as a proxy for storm-local upper-tropospheric temperatures.

Data and method

Previous work has focused on time series of potential intensity from annual averages over specified fixed regions (e.g., Emanuel et al. 2013; Vecchi et al. 2013). These regions typically reflect the "main development regions" of tropical cyclones or may span the entire tropics. Here a historical global record of tropical cyclone tracks is used to navigate through the reanalysis data and estimate the actual local environmental conditions that the storms experienced during their lifetimes (Kossin and Camargo 2009).

For every 3-hour period during each storm's lifetime, the time and position of the storm center (typically called a "storm-fix") is used to estimate the environmental conditions from each reanalysis product. The storm-fixes are taken from the Advanced Dvorak Technique–Hurricane Satellite (ADT-HURSAT) data record (Kossin et al. 2013), which is based on interpolated and re-centered fixes from the International Best Track Archive for Climate Stewardship (IBTrACS;

Knapp et al. 2010), and presently spans the period 1982–2009. Reanalysis data are taken from monthly-mean fields. The MERRA, ERA-Interim, and NCEP/NCAR data are provided, respectively, on 2/3° × 0.5°, 1.5° × 1.5°, and 2.5° × 2.5° longitude × latitude grids. Potential intensity and outflow temperature were calculated from the reanalysis data following Bister and Emanuel (1998).

The storm-local environmental conditions are estimated by linearly interpolating the monthly-mean reanalysis fields to the time of the storm-fix and taking the value in the grid-box that contains the storm-center position at that time. These values are then averaged annually. The resulting time series are more relevant for questions regarding detection and attribution of past observed changes in tropical cyclone intensity because potential intensity trends in regions that have not experienced the passage of a tropical cyclone are not directly physically linked to observed tropical cyclone intensity variability or trends through potential intensity theory (Kossin and Camargo 2009). Using daily or 6-hourly reanalysis fields does not appreciably change the results shown here, and the National Centers for Environmental Prediction / Department of Energy Reanalysis 2 (NCEP/DOE; Kanamitsu et al. 2002) gives essentially the same result as the NCEP/NCAR data.

Following the storm tracks, the ADT-HURSAT data record is used to identify mature tropical cyclones that are at least Category-1 in strength (maximum near-surface wind speed > 33 m s^{-1}). This results in about 23,300 3-hourly storm fixes in about 1,100 storms globally over the period 1982–2009. Annually averaged satellite infrared cloud-top brightness temperatures were reduced by 8°C in the time series shown in Figs. 4 and 5. This warm bias is expected and is due to the optical properties of the clouds being measured (e.g., Holz et al. 2006). Confidence intervals for the trends shown in Figs. 2 and 4 were calculated after testing the time series for serial correlation using a Durbin-Watson test (Wilks 2006). All trends are based on ordinary least squares.

Results

Time series of the annual-mean storm-local potential intensity calculated from the MERRA, ERA-Interim, and NCEP/NCAR data are shown in Fig. 2. There are clear biases in the mean between the potential intensity calculated from the three products, with the NCEP/NCAR exhibiting the lowest mean and the ERA-Interim the greatest. Of greater relevance to the detection and attribution of global trends in tropical cyclone intensity, the NCEP/NCAR data exhibit a statistically significant increasing trend, but no trends are found in the MERRA or ERA-Interim data.

As noted above, potential intensity is strongly correlated with sea surface temperature and temperatures near the atmospheric tropopause. In potential intensity theory, the near-tropopause temperature represents “outflow temperature”, which is the local environmental temperature near the height where central updrafts of a mature tropical cyclone would diverge outwards away from the storm center (Bister and Emanuel 1998; Emanuel 1999). Following the storms, the annual-mean sea surface temperatures used by the three reanalysis products all exhibit very similar variability and trends (Fig. 3), so sea surface temperature differences cannot be implicated for the disparity in potential intensity trends seen in Fig. 2.

For each of the roughly 23,300 3-hourly storm fixes, the HURSAT dataset has a satellite infrared image centered on the storm (Knapp and Kossin 2007). Mature tropical cyclones of Category-1 strength or greater typically maintain vigorous and persistent updrafts near their centers. The updrafts reach heights near the tropopause where they then diverge outward away from the center, and the local atmospheric temperature at this height is the outflow temperature of

the storm. The temperatures of the tops of the clouds can be estimated using infrared radiances measured by satellite sensors that are converted to brightness temperatures.

Time series of annually-averaged satellite-measured cloud-top and storm-local outflow temperatures calculated using the three reanalysis products are shown in Fig. 4. The MERRA and ERA-Interim outflow temperature time series are significantly correlated with the satellite-measured cloud-top temperature time series with Pearson coefficient of $r \sim 0.8$. The NCEP/NCAR time series is significantly correlated with coefficient $r \sim 0.5$ ($r \sim 0.7$ when detrended). The most striking difference in the time series from the three products is the statistically significant cooling trend in the NCEP/NCAR outflow temperatures, which is not found in the MERRA or ERA-Interim series. In the storm-local framework, it is evident that the upper-level outflow temperature differences can be implicated for the differences in potential intensity trends (Fig. 2), which is in agreement with results based on regionally averaged temperatures (e.g., Emanuel et al. 2013; Vecchi et al. 2013). But here, these trends can be compared to outflow temperature trends deduced directly from satellite cloud-top temperatures (black line in Fig. 4).

The lack of any coincident trend in the cloud-top temperatures provides compelling supporting evidence that the trends in the NCEP/NCAR-derived upper-level outflow temperatures and potential intensity are spurious. The agreement in the lack of trends between the cloud-top temperatures and the MERRA and ERA-interim time series further suggests that this is most likely representative of how the mean storm-local environment and potential intensity has varied in the past 30 years. This has important implications because a lack of storm-local potential intensity trend implies that there is no manifest expectation within the constructs of potential intensity theory that mean tropical cyclone intensity has increased over the past 30 years. This somewhat complicates the interpretation of observed global intensity trends over this same period (e.g., Elsner et al. 2008; Kossin et al. 2013) and their underlying causes.

Agreement among the reanalysis products and between the products and the satellite-measured cloud-top temperatures varies among the different ocean basins (Fig. 5). Agreement is best in the North Atlantic where there is consistent outflow temperature cooling, although this cooling is apparently exaggerated in the NCEP/NCAR data. This is also the only basin with clear and substantial trends in hurricane intensity using the most recent satellite reanalysis of global tropical cyclone intensity (ADT-HURSAT; Kossin et al. 2013) over the same period. The mean storm cloud-top temperatures and the storm-local outflow temperatures from the MERRA and ERA-Interim show a general warming trend in the western and eastern North Pacific while the NCEP/NCAR data show a cooling trend. In the Northern Indian Ocean and the Southern Hemisphere, the mean storm cloud-top temperatures and the storm-local outflow temperatures from the MERRA and ERA-Interim show no trend while the NCEP/NCAR data show a cooling trend.

Part of the variability found in the storm-local outflow temperature and potential intensity time series is due to variability of the storm tracks in the presence of environmental gradients. For example, upper-level temperatures in the tropics generally increase poleward of the equator and potential intensity generally decreases, so that variability of the mean latitude of the storm tracks will cause variability in the mean storm-local environment even if the environment is constant in time (Kossin and Camargo 2009). Alternatively, variability in the storm-local environment can be caused by temporal changes in the environment in the absence of any mean track changes. In reality, both of these factors contribute to the variability of the storm-local environment. This is shown in Fig. 6.

To create Fig. 6a, the global potential intensity fields for each month were averaged over the entire period shown and the storm tracks were then navigated through the averaged fields from

each reanalysis product. This conserves the seasonal cycle of potential intensity but removes any interannual variability or trend. When this is done, trends from the three reanalysis products are in much better agreement (cf. Fig. 2), and are all essentially flat. To create Fig. 6b, each of the roughly 23,300 storm fixes is assigned a random year from the entire period shown. This conserves interannual variability and trends in the environment and allows the tracks to vary within their observed range and seasonality, but removes any trends from the longer-term track characteristics. When this is done, the three reanalysis products all exhibit increases in storm-local potential intensity. This can be explained by the recent observation that the average latitude where tropical cyclones reach their peak intensity has migrated poleward over the same period (Kossin et al. 2014). It appears from Figs. 2 and 6 that this poleward migration has caused the mean storm-local potential intensity to decrease at roughly the same rate that the potential intensity mean state is increasing in the regions where storms track (Fig. 1). The lack of global storm-local PI trends is thus due to a balance between temporal increases in the mean state and the poleward migration of tropical cyclones into lower climatological potential intensity.

Summary

By using tropical cyclones as thermometers that can measure upper-tropospheric temperatures, a significant source of uncertainty in past global trends in the tropical cyclone environment is mitigated. The upper-level cooling trend found in the NCEP/NCAR reanalysis data appears to be spurious, and consequently the associated increasing trend in tropical cyclone potential intensity is also very likely spurious. The lack of trends in the local environment that the tropical cyclones have tracked through in the past 30 years, as measured with the MERRA and ERA-Interim data, is validated by upper-tropospheric temperature information provided by the tropical cyclones themselves.

The lack of a global trend in mean storm-local potential intensity suggests that there is no manifest theoretical expectation that global-mean tropical cyclone intensity has increased in the past 30 years, at least based on potential intensity theory. This is consistent with observations that mean tropical cyclone lifetime-maximum intensity exhibits no significant trend over this period (Elsner et al. 2008; Kossin et al. 2013). Trends in other storm-local environmental factors, such as vertical wind shear, can provide an alternative basis for an expectation of intensity trends, but these were not explored here. The lack of trends in mean storm-local potential intensity is not due to a lack of temporal changes in the environment, but appears to be due to the offsetting effect of the poleward migration of tropical cyclones that has occurred over this same period (Kossin et al. 2014).

References

Bister, M., and K. A. Emanuel, 1998: Dissipative heating and hurricane intensity. *Meteor. Atmos. Phys.*, **65**, 233–240.

Christensen, J. H., and Coauthors, 2013: Climate Phenomena and their Relevance for Future Regional Climate Change. *Climate Change 2013: The Physical Science Basis. Contribution of Working Group I to the Fifth Assessment Report of the Intergovernmental Panel on Climate Change*, T. F. Stocker et al., Eds., Cambridge University Press, 1217–1308.

Dee, D.P., and Coauthors, 2011: The ERA-Interim reanalysis: configuration and performance of the data assimilation system, *Quart. J. Roy. Meteor. Soc.*, **137**, 553–597.

Elsner, J. B., J. P. Kossin, and T. H. Jagger, 2008: The increasing intensity of the strongest tropical cyclones. *Nature*, **455**, 92–95.
Emanuel, K. A., 1999: Thermodynamic control of hurricane intensity. *Nature*, **401**, 665–669.
Emanuel, K. A., 2000: A statistical analysis of hurricane intensity. *Mon. Wea. Rev.*, **128**, 1139–1152.
Emanuel, K., S. Solomon, D. Folini, S. Davis, and C. Cagnazzo, 2013: Influence of tropical tropopause layer cooling on Atlantic hurricane activity. *J. Climate*, **26**, 2288–2301.
Holz, R. E., S. Ackerman, P. Antonelli, F. Nagle, and R. O. Knuteson, 2006: An improvement to the high-spectral-resolution CO_2-slicing cloud-top altitude retrieval. *J. Atmos. Oceanic Technol.*, **23**, 653–670.
Kalnay, E., and Coauthors, 1996: The NCEP/NCAR 40-year reanalysis project. *Bull. Amer. Meteor. Soc.*, **77**, 437–470.
Kanamitsu, M., W. Ebisuzaki, J. Woollen, S-K Yang, J. J. Hnilo, M. Fiorino, and G. L. Potter, 2002: NCEP-DOE AMIP-II Reanalysis (R-2). *Bull. Amer. Meteor. Soc.*, **83**, 1631–1643.
Knapp, K. R., and J. P. Kossin, 2007: A new global tropical cyclone data set from ISCCP B1 geostationary satellite observations. *J. Appl. Remote Sens.*, **1**, 013505, DOI:10.1117/12.731296.
Knapp, K. R., M. C. Kruk, D. H. Levinson, H. J. Diamond, and C. J. Neumann, 2010: The International Best Track Archive for Climate Stewardship (IBTrACS): Unifying tropical cyclone best track data. *Bull. Amer. Meteor. Soc.*, **91**, 363-376.
Knutson, T. R., and Coauthors, 2010: Tropical cyclones and climate change. *Nat. Geosci.*, **3**, 157–163.
Kossin, J. P., and S. J. Camargo, 2009: Hurricane track variability and secular potential intensity trends. *Climatic Change*, **97**, 329–337.
Kossin, J. P., T. L. Olander, and K. R. Knapp, 2013: Trend analysis with a new global record of tropical cyclone intensity. *J. Climate*, **26**, 9960–9976.
Kossin, J. P., K. A. Emanuel, and G. A. Vecchi, 2014: The poleward migration of the location of tropical cyclone maximum intensity. *Nature*, **509**, 349–352.
Rienecker, M., and Coauthors, 2011: MERRA: NASA's Modern-Era Retrospective Analysis for Research and Applications, *J. Climate*, **24**, 3624–3648.
Seneviratne, S. I., and Coauthors, 2012: Changes in climate extremes and their impacts on the natural physical environment. *Managing the Risks of Extreme Events and Disasters to Advance Climate Change Adaptation*, C. B. Field et al., Eds., Cambridge University Press, 109–230.
Vecchi, G. A., S. Fueglistaler, I. M. Held, T. R. Knutson, and M. Zhao, 2013: Impacts of atmospheric temperature trends on tropical cyclone activity. *J. Climate*, **26**, 3877–3891.
Wilks, D. S., 2006: *Statistical Methods in the Atmospheric Sciences*. 2nd ed. International Geophysics Series, Vol. 91, Academic Press, 627 pp.

Acknowledgements: This work benefitted greatly from discussions with Kerry Emanuel (MIT) and Gabriel Vecchi (NOAA/GFDL). Potential intensity outflow temperature data were generously provided by Kerry Emanuel. NCEP/NCAR Reanalysis-1 and NCEP/DOE Reanalysis-2 data were provided by the NOAA/OAR/ESRL PSD, Boulder, Colorado, USA, from their website at http://www.esrl.noaa.gov/psd/. ERA-Interim data were provided by the European Centre For Medium-Range Weather Forecasts (ECMWF) via their web portal at http://apps.ecmwf.int/datasets/. MERRA data were provided by the Global Modeling and Assimilation Office (GMAO) at NASA Goddard Space Flight Center through the NASA GES DISC online archive via their web portal at http://gmao.gsfc.nasa.gov/merra/.

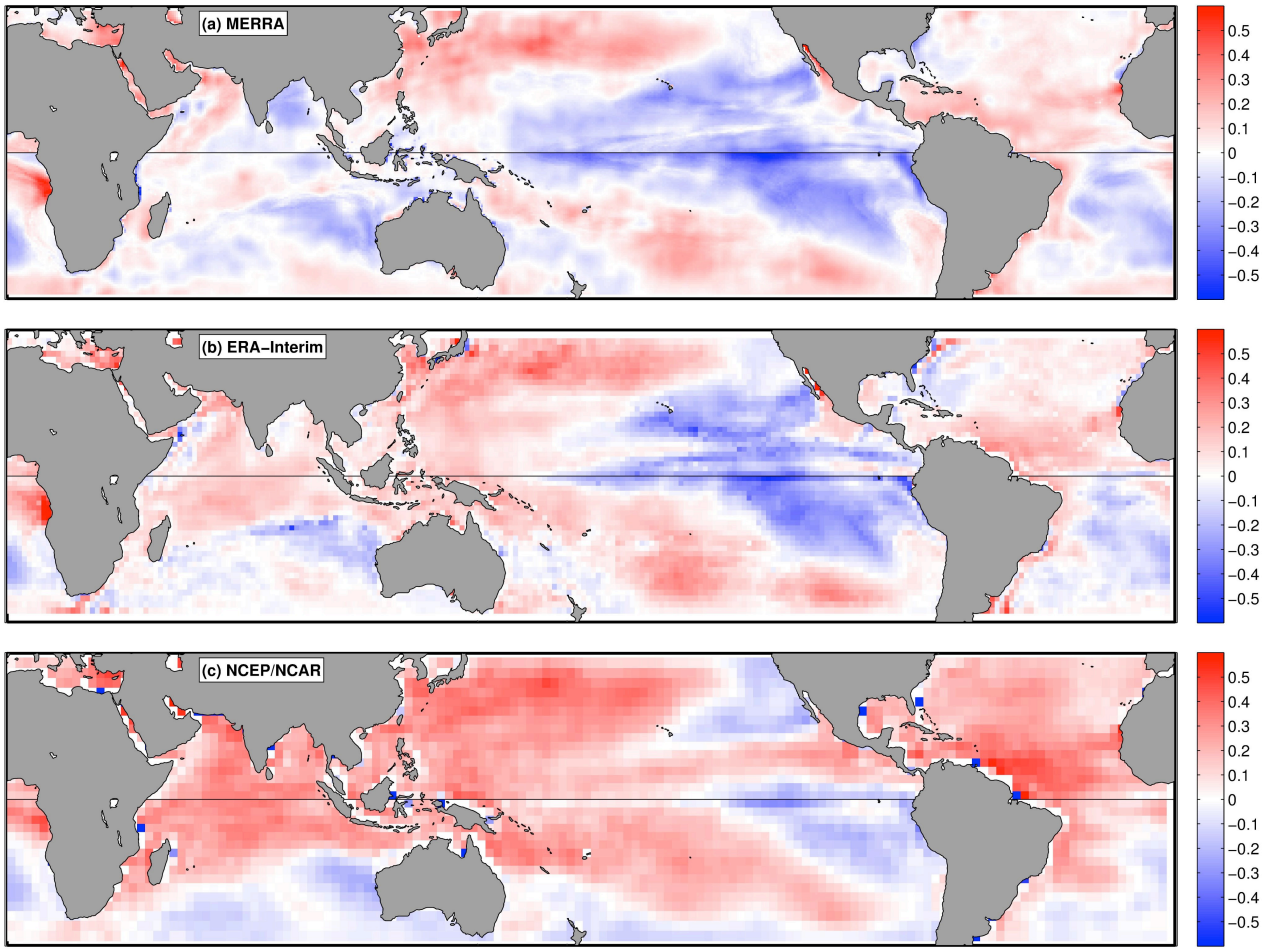

Figure 1: Tropical cyclone potential intensity trends in m s^{-1} per year over the period 1980–2010 calculated from the (a) MERRA, (b) ERA-Interim, and (c) NCEP/NCAR reanalysis products. Trends are based on annual values averaged over August–October in the Northern Hemisphere and January–March in the Southern Hemisphere.

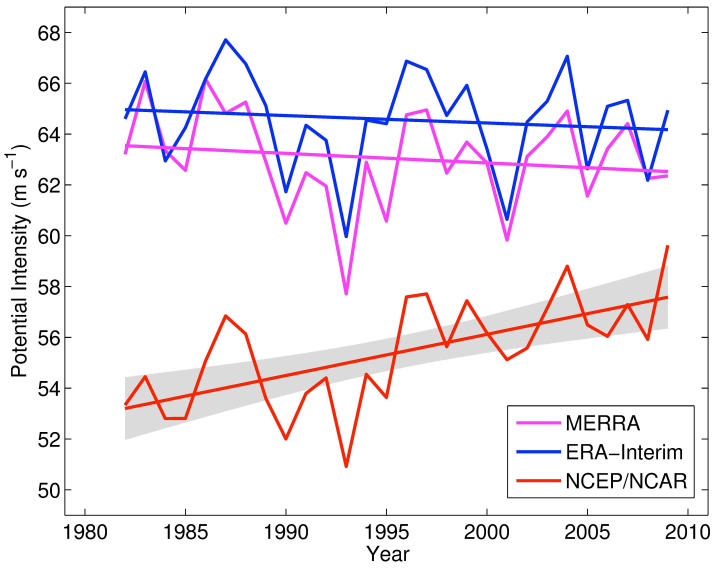

Figure 2: Time series of annual-mean storm-local potential intensity and their linear trends. Based on MERRA (magenta), ERA-Interim (blue), and NCEP/NCAR (red). Grey shading represents the 95% two-sided confidence interval of the NCEP/NCAR trend. The MERRA and ERA-Interim trends are not statistically significant.

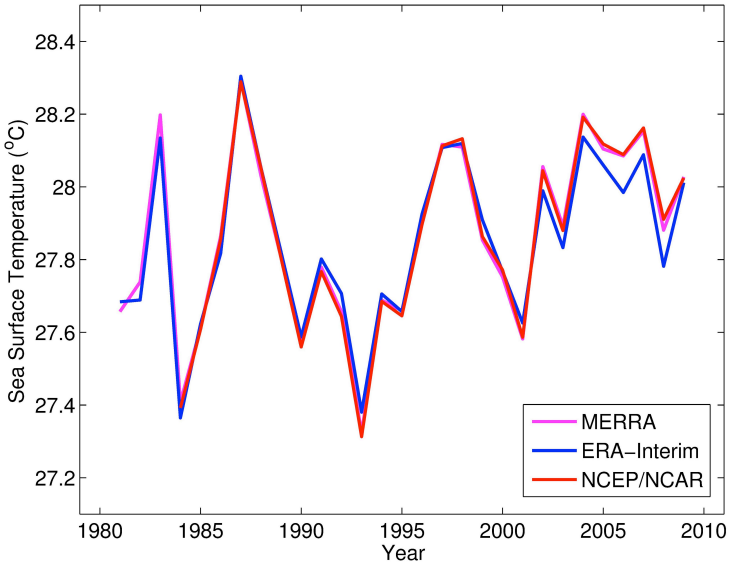

Figure 3: Time series of annual-mean storm-local sea surface temperatures. Based on MERRA (magenta), ERA-Interim (blue), and NCEP/NCAR (red).

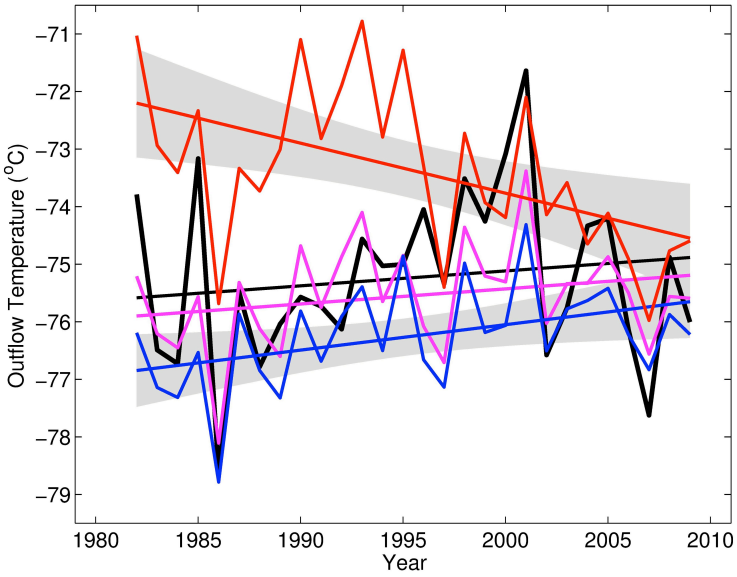

Figure 4: Time series of annual-mean storm-local outflow temperatures and their linear trends. Based on MERRA (magenta), ERA-Interim (blue), NCEP/NCAR (red), and tropical cyclone cloud-top temperature from satellite-measured infrared brightness temperature (black). The satellite-measured brightness temperatures have been reduced by 8°C for plotting purposes (see Data and method section). Grey shading represents the 95% two-sided confidence interval of the NCEP/NCAR cooling trend and ERA-Interim warming trend. The MERRA and infrared brightness temperature trends are not statistically significant.

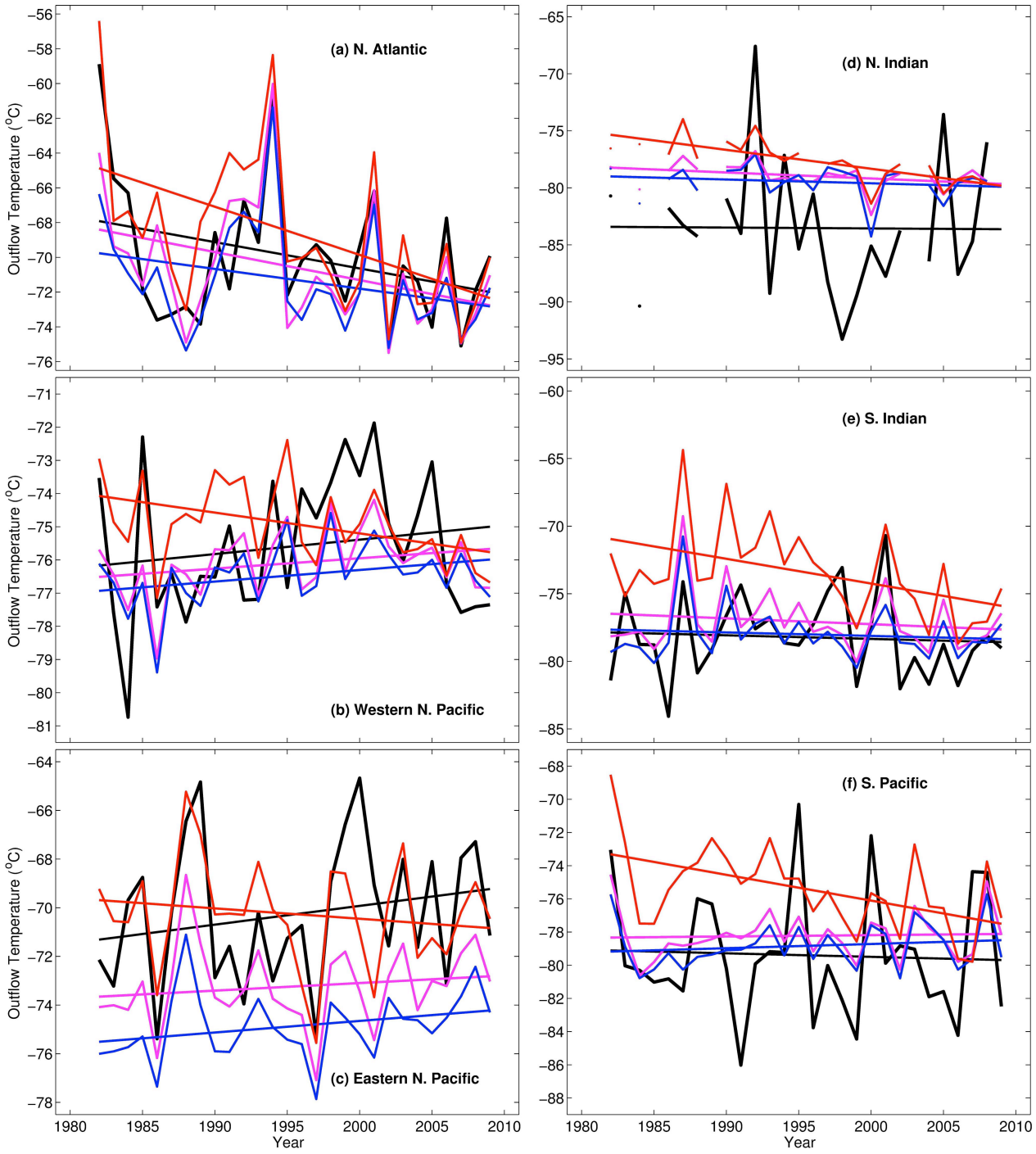

Figure 5: Similar to Fig. 4, but following tropical cyclones in the (a) North Atlantic, (b) western North Pacific, (c) eastern North Pacific, (d) Northern Indian Ocean, (e) Southern Indian Ocean, and (f) South Pacific. Missing annual values in the Northern Indian Ocean are due to a lack of Category-1 strength storms for those years.

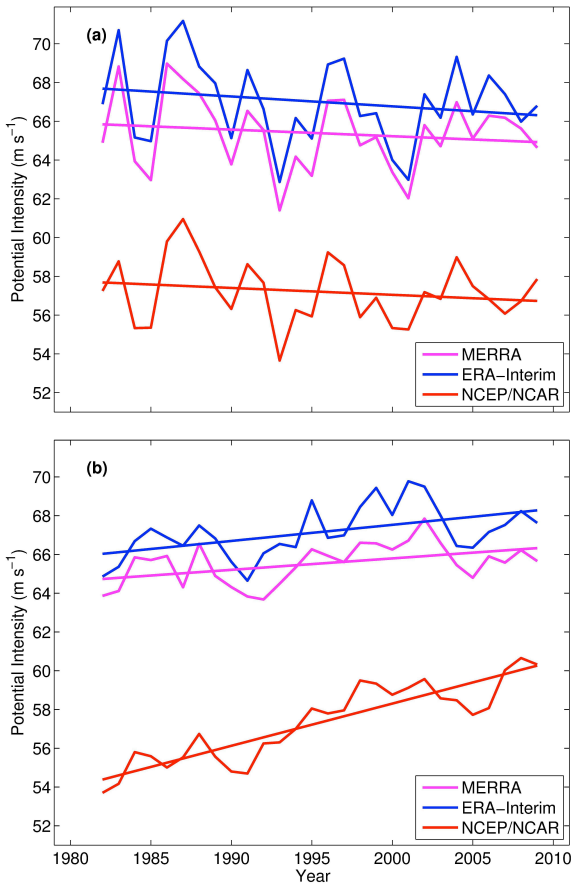

Figure 6: Similar to Fig. 2, but with (a) environmental trends removed and (b) trends in the track characteristics removed.